

Application of the Transient Hot-Wire Technique to the Measurement of the Thermal Conductivity of Solids

M. J. Assael,^{1,2} M. Dix,³ K. Gialou,¹ L. Vozar,⁴ and W. A. Wakeham³

Received August 30, 2001

A novel application of the transient hot-wire technique for thermal conductivity measurements is described. The new application is intended to provide an accurate means of implementation of the method to the determination of the thermal conductivity of solids exemplified by a standard reference ceramic material. The methodology makes use of a soft-solid material between the hot wires of the technique and the solid of interest. Measurements of the transient temperature rise of the wires in response to an electrical heating step in the wires over a period of 20 μ s to 10 s allows an absolute determination of the thermal conductivity of the solid. The method is based on a full theoretical model with equations solved by finite-element method applied to the exact geometry. The uncertainty achieved for the thermal conductivity is better than $\pm 1\%$, and for the product (ρC_p) about $\pm 3\%$. The whole measurement involves a temperature rise less than 4 K.

KEY WORDS: ceramic; solid; thermal conductivity; transient hot-wire.

1. INTRODUCTION

During the last two decades the transient hot-wire technique has successfully been applied to the measurement of the thermal conductivity of gases [1] and liquids [2] over a very wide range of temperatures and pressures, excluding the critical region. Indeed, the technique has now been recognized [3] as an absolute technique able to measure the thermal conductivity of

¹ Chemical Engineering Department, Aristotle University, 54006 Thessaloniki, Greece.

² To whom correspondence should be addressed. E-mail: assael@transp.eng.auth.gr

³ Department of Chemical Engineering and Chemical Technology, Imperial College of Science, Technology and Medicine, London SW2 2BY, United Kingdom.

⁴ Physics Department, Constantine the Philosopher University, Nitra, Slovakia.

fluids with an uncertainty of about $\pm 0.5\%$. In the case of fluids, two thin wires have been employed to eliminate end effects, acting as the transient heating source and at the same time as a thermometer registering the fluid temperature rise at the wire surface. Typical temperature rises are about 3 K attained in a time of about 1 s.

The application of the technique to the measurement of the thermal conductivity of solids has not, however, been that successful. Four main variations of the technique can be found in the literature:

- (a) The oldest variation is that initially employed by Haupin [4] in 1960, whereby a thermocouple with its junction placed in the middle of the sample, is heated with an alternating current. At the same time, a filter network is used to eliminate the ac heating current, allowing the thermocouple emf to be measured.
- (b) The second method was developed by Mittenbühler [5] and formed the basis of methods for a German standard [6] and a European standard [7] in use today. The method employs a heating wire of one metal with a thermocouple welded to the heating wire in the form of a cross. An ac or dc power source can be employed, and the temperature rise generated by a known heating power is used to determine the thermal conductivity.
- (c) The parallel method, also adopted as a European standard [8] in 1998, places the thermocouple some distance from the heating wire (usually about 1 mm). The theory of the method is therefore slightly different but the principle remains the same. A variation of this method is the probe method according to which the wire and the thermocouple are placed in a ceramic tube [9] and the ceramic tube itself is placed inside the solid material.
- (d) All the aforementioned methods employ a thermocouple for the temperature measurement and hence measure only at one point. To obtain a better average measurement of the temperature, the resistance of the heating wire can be recorded during the measurement [10]. Thus, the wire acts both as the heating source and as a thermometer. This is generally achieved employing a resistance bridge.

All four methods are characterized by similar problems:

- (i) To avoid problems of thermal resistance, the wire (and the thermocouple) are placed in a groove on the surface of a block of the solid while another block of the solid is placed over them. Both solid surfaces have to be very flat while powder from the solid takes up the empty space between the wire and groove.

- (ii) The above arrangement still produces a contact resistance, so large temperature rises of 10 to 20 K are usually employed coupled with large time scales, i.e., usually 1 to 10 min, so that temperature gradients are reduced. This means that large blocks of solids must be used so that the temperature front does not meet the outer extremes of the solid.
- (iii) To obtain the thermal conductivity, an approximate analysis is employed. The thermal conductivity is obtained from the slope of a straight portion of the temperature rise vs. the logarithm of the time curve. Laborious analyses have been employed [11] to define this straight portion in the temperature rise curve.
- (iv) The use of large diameter heater and thermocouple wires, of which appropriate account is not taken and variations of heater current [12], have resulted in large discrepancies among the results.
- (v) Finally, it should be emphasized that none of the methods has been supported by a rigorous absolute theory.

The uncertainty of the above methods ranges to about 5 to 10%.

Other applications of wires to the measurement of the thermal conductivity have made use of a spiral wire to generate a plane source of heat, for which the one-dimensional theory is often adequate to permit reliable relative measurements [13]. However, that application is more similar to a transient hot disc rather than the transient hot wire considered here.

The present paper will describe a novel approach that, backed by a fully developed theoretical model and elimination of the above problems, is able to measure the thermal conductivity of solids with an absolute uncertainty of better than $\pm 1\%$, at least, in the case of the ceramics to which it is applied here for the first time.

2. THEORETICAL

2.1. Fundamental Equations

In the transient hot-wire technique, the temporal rise of a thin wire immersed in a test material, initially at thermal equilibrium, is observed following the application of a step voltage across the wire. The wire acts as a heat source and produces a time-dependent temperature field within the test material. When measurements are carried out in such a way as to minimize radiative effects and the material is isotropic with temperature-

independent thermal conductivity, density, and heat capacity, the temperature gradient is described by the equation

$$\rho C_p \frac{\partial T}{\partial t} = \lambda \nabla^2 T \quad (1)$$

where, ρ , C_p , and λ are the density, the isobaric heat capacity, and the thermal conductivity of the test material, while T is the absolute temperature.

The geometry of the transient hot wire proposed here for the measurement of the thermal conductivity of solids is shown in Fig. 1. The wire is placed between two semi-infinite blocks of solid of width “ b .” Between the wire and the solid, it will be assumed that there is a thin layer of another material; this is maybe air (if no attempt is made to eliminate contact resistance) or a soft solid such as silicone paste (if such attempts are made). Equation (1) must be applied to three distinct regions: to the wire (subscript “w”), to the intermediate layer (subscript “m”), and to the solid (subscript “s”). It is assumed that, from an initial equilibrium state in which $T = T_0$ everywhere, heat is generated in the wire at a rate q per unit length. The system is considered infinitely long along the wire axis, and that in essence, the solid blocks are large enough to be considered as infinite in the x and y directions. The full set of equations is shown in Appendix A,

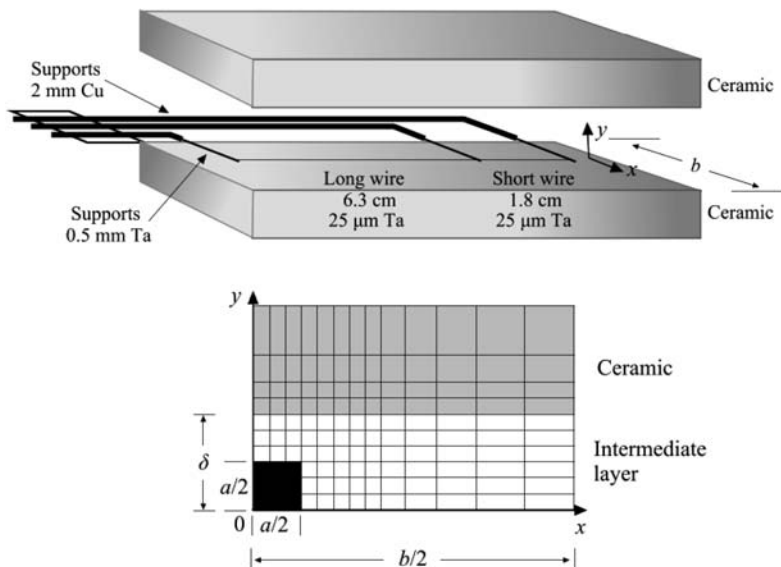


Fig. 1. Schematic diagram of the two-wire sensor.

Table AI, while in Table AII the same equations are also shown in dimensionless form. There is no analytic solution of these equations, and they are to be solved by a two-dimensional finite-element analysis.

In order to make this finite-element solution rapid and accurate, we employ a representation of the circular wire by a square of side " a ," so that we may use rectangular coordinates everywhere, as has been demonstrated [14] that this representation is quite sufficient to secure high accuracy in the theoretical description of the temperature rise of a circular cross-section wire in similar circumstances. This is also demonstrated in Appendix B, where the aforementioned representation of the wire as a mesh of rectangular elements, is compared with a more precise mesh, which is a combination of both triangular and rectangular elements. Both arrangements, when employed in the analysis of liquid toluene data, produced the same value of the thermal conductivity within its uncertainty. Hence, the first arrangement was preferred due to its speed of conversion.

To solve the aforementioned equations, a 441 element, 2-D rectangular variable size mesh is assumed. The mesh in the wire, as well as in the intermediate layer and in the two interfaces, is quite dense. The elements' size increases inside the solid the further they are located from the interface.

3. EXPERIMENTAL

3.1. The Wire Sensor

The aforementioned equations refer to the temporal temperature change of the wire-intermediate layer-solid system. To measure this temperature rise, the resistance of the heating wire itself is recorded. Furthermore, as will be discussed later, two identical wires differing only in length are employed. This arrangement corresponds to the resistance change of a finite segment of an infinitely long wire [15].

The two-wire arrangement employed for the present measurements of the thermal conductivity at atmospheric pressure is shown in Fig. 1. The two wires, placed one after the other, are made out of 25- μm -diameter tantalum and have lengths of 6.3 cm and 1.8 cm, respectively. They are spot welded to flattened 0.5-mm-diameter tantalum wire supports, which in turn are connected to thick copper rod contacts. To heat the wires and measure their resistance at the same time, an automatic bridge controlled by a computer was employed.

3.2. Measurement Bridge Circuit

As already discussed, the purpose of employing the electronic bridge in the transient hot-wire instrument is twofold: first, to measure the evolution

of the resistance change of a finite segment of infinite wire (by automatically compensating for axial heat conduction from the wire ends), and second, to ensure that a known constant heat flux is generated in the hot wires.

This is achieved by placing two identical wires of different length and resistance in the two arms of a Wheatstone-type bridge circuit (Fig. 2). In this way the bridge becomes sensitive to the difference in resistance of the two wires, which is equivalent to the resistance of a segment of an infinite wire. The temperature rise, which is required to calculate the thermal conductivity, can then be calculated from the temperature—resistance characteristics of the hot wires.

The principal characteristics of the bridge circuit are:

- the direct measurement of the out-of-balance voltage during the transient run,
- the ability to begin measurements from $20 \mu\text{s}$ after the initiation of heating and to obtain a large number of data points, and
- a temperature resolution of 5 mK and time resolution of $1 \mu\text{s}$.

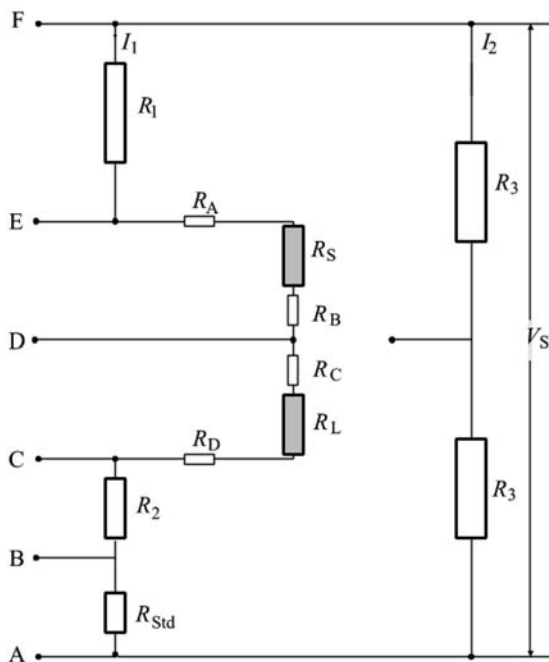


Fig. 2. The bridge circuit.

A transient measurement run is initiated by adjusting the variable resistors R_1 and R_2 (Resistance Box RBC5A, Cropico Ltd., UK) using a low voltage (0.5 V); typically, $R_1 \approx R_L$ and $R_2 \approx R_S$, where R_L and R_S are the resistances of the long and short wire (Fig. 2). R_A , R_B , R_C , and R_D (Fig. 2) denote the lead resistances of the two wires, respectively. Balancing of the bridge is performed corresponding to the zero-voltage level set by two identical resistors R_3 . Simultaneous switching on two MOSFET switches then activates the bridge. This applies a constant voltage across the bridge circuit, which is supplied from a dc programmable dual power supply (TSP3222, Thurbly Thandar Ltd., UK). The output signal of the bridge is then preamplified, converted by an analogue-to-digital (A/D) converter (24-bit, 16-channel multiplexed conversion, PC30AT Amplicon Liveline Ltd., UK), and then the data points are subsequently stored in the computer that controls the measurement. A data acquisition program drives the electronics and automates the transient measurement.

In the bridge, two MOSFET switches have been employed to symmetrically switch on (~ 100 – 200 ns) the bridge about earth ground. This reduces the common-mode transient signal (< 20 mV) at the sensing terminals of the bridge to a level where measurements can begin $20 \mu\text{s}$ after the initiation of the experiment. The resulting reduction of the common mode signal allows the differential amplifier to be connected directly to the bridge without causing saturation overload. The differential amplifier also acts as a “buffer” between the bridge and the external measuring electronics, which prevents the introduction of noise into the bridge circuit itself. The A/D converter has a maximum conversion rate of 50 kHz ($20 \mu\text{s}$) and a precision in time of $\pm 1 \mu\text{s}$. It enables a large number of data points to be obtained over the measurement interval, in fact, more than can be practically analyzed.

A seven-digit high-resolution digital voltmeter (HP 34401A, Hewlett Packard), capable of 1000 readings per second, is also used. Its function is threefold: first, it is used to measure the supply voltage during the transient run, second, it is used to measure the voltage across the bridge resistances during the steady-state run, including a standard resistor $R_{\text{Std}} = 10 \Omega$ (Tinsley), which provides a reference for the measurements, and third, it is used to calibrate the A/D converter.

3.3. Working Equations

The bridge circuit, shown in Fig. 2, has been designed to measure the evolution of the resistance change of a finite portion of an infinite wire, by automatically compensating for wire ends, and to generate a nearly constant heat flux in the hot wires of known magnitude. In this section, the working bridge equations are derived from an analysis of the circuit.

By placing two identical wires of different length in the arrangement shown in Fig. 2, it is possible to compensate for the wire ends, as the bridge is arranged to calculate the difference of the resistances of the two wires and, thus, wire-end resistances are cancelled out. That is, if we assume that the wires have identical ends and the lead resistances of the two wires are also the same,

$$R_A + R_C = R_B + R_D \quad (2)$$

then, by solving the bridge circuit, the expression for the change in resistance of a hypothetical segment of an infinite “working” wire $\Delta R_W(t) = R_W(t) - R_W(0)$ as a function of time t can be expressed as

$$\Delta R_W(t)$$

$$= \frac{\frac{\Delta V_{CE}(t)}{V_S} \Sigma R(0)^2}{\Sigma R(0) \left(1 + \frac{R_S(0)}{R_W(0)}\right) - R_F(0) \left(1 + 2 \frac{R_S(0)}{R_W(0)}\right) - \frac{\Delta V_{CE}(t)}{V_S} \Sigma R(0) \left(1 + 2 \frac{R_S(0)}{R_W(0)}\right)} \quad (3)$$

where $R_W(t)$ and $R_W(0)$ denote the resistance of the “working” wire at any time and at zero time ($t=0$), respectively, defined as

$$R_W(t) = R_L(t) - R_S(t) \quad (4)$$

and

$$R_W(0) = R_L(0) - R_S(0) \quad (5)$$

In the above equations, $R_L(t)$ and $R_L(0)$ are the resistances of the long wire at time t and at zero time ($t=0$), $R_S(t)$ and $R_S(0)$ are the resistances of the short wire at time t and at zero time ($t=0$), $\Delta V_{CE}(t)$ is the measured out-of-balance voltage, and V_S is the supply voltage. $\Sigma R(0)$ is the sum of the resistances of the left-hand side of the circuit at zero time, as

$$\Sigma R(0) = R_1 + R_A + R_S(0) + R_B + R_C + R_L(0) + R_D + R_2 + R_{Std} \quad (6)$$

and $R_F(0)$ is the sum of the bottom arm resistances,

$$R_F(0) = R_C + R_L(0) + R_D + R_2 + R_{Std} \quad (7)$$

Equation (3) implies that by implementing the present bridge design, shown in Fig. 2, it is possible to calculate the resistance change for a

hypothetical segment of an infinite wire with the knowledge of the following information:

- (a) the ratio of the out-of-balance voltage and the supply voltage $\Delta V_{CE}(t)/V_S$ at time t ,
- (b) the total resistance of the left-hand arm of the circuit $\Sigma R(0)$ and the bottom arm resistance $R_F(0)$ at zero time, and
- (c) the ratio of the short to the “working” wire resistance $R_S(0)/R_W(0)$ at zero time.

Over the small temperature interval (about 3 K) of the measurement, the temperature rise of the hot wire can be expressed as

$$\Delta T = \frac{\Delta R_W(t)}{\alpha_L(T, T_0) R_W(0)} \quad (8)$$

where $\alpha_L(T, T_0)$ is the pseudo-linear-temperature coefficient of resistance, obtained as

$$\alpha_L(T, T_0) = \frac{\alpha + \beta[2(T - 273.15) - (T - T_0)]}{1 + \alpha(T_0 - 273.15) + \beta(T_0 - 273.15)^2} \quad (9)$$

where the initial temperature is taken as the reference temperature T_0 , and α and β are the first and second temperature-resistance coefficients of the material of the wires.

The above analysis presupposes the generation of a constant heat flux within the long and short wire. The implication in this statement is that the same constant current must therefore flow through both wires. Since the resistance of both wires is changing with time, the current also necessarily changes. However, the change in the resistance difference of the two wires, over a single-measurement interval, is of the order of 10^{-3} Ohm. This corresponds to a change of current, of the order of 10^{-6} A (assuming $\Sigma R(0) \approx 50$ Ohm, and $V_S \approx 5$ V), which in turn results to a change of the heat flux per unit length of the order of 10^{-6} W · m⁻¹ (when typical values of heat flux per unit length employed are about 3 W · m⁻¹). Hence, both the heat flux per unit length and the current, can safely be considered as constants.

Thus, the same current I_1 flows through both wires. Analyzing the bridge circuit it can be shown that the heat flux per unit length of the middle portion of the long wire, at any instant t , can then be expressed as

$$q = \frac{V_S^2}{\left\{ R_1 + R_A + R_B + R_C + R_D + R_2 + R_{Std} + \frac{R_W(t)(L_L + L_S)}{L_L - L_S} \right\}^2} \frac{R_W(t)}{L_L - L_S} \quad (10)$$

where L_L and L_S are the lengths of the long and short wires, respectively. Finally, we should note that as a result of the manufacturing process of “thin” hot wires (and the wire supports), it is difficult to ensure that the cross section of the two wires is uniform, which may result in a small variation in the resistance per unit length of the wires. A small correction is hence applied to the measured temperature rise and heat flux, as described elsewhere [15]. At any specific time, from the resistance measurement of the bridge the temperature rise of a section of the wire is calculated via Eq. (8).

Using the finite element solution outlined above, an estimate of the theoretical temperature rise of the wire may be generated from assumed values of λ and (ρC_p) for tantalum, for the intermediate layer, and for the test solid, given the dimensions of the wire, the thickness δ of the intermediate layer and the heat input to the wire. In practice λ , and (ρC_p) of tantalum are known so that for a given measurement there are five unknown quantities:

- (a) the thermal conductivity λ_s , and the product $(\rho_s C_{ps})$ for solid and
- (b) the thermal conductivity λ_m , the product $(\rho_m C_{pm})$, and the thickness of the intermediate layer.

Adjustment of all five variables leads to their evaluation, when the theoretical curve is brought into coincidence with that experimentally determined. In practice, the characteristics of the intermediate layer are evaluated from measurements at very short time, whereas those of the solid are derived essentially independently from results at longer times. The five quantities are uniquely determined because some thousand measurements of the temperature rise are accumulated during one run.

3.4. Steady-State Measurement

In order to measure the temperature rise during a run, the total resistance of the left-hand arm of the circuit $\Sigma R(0)$, the bottom arm resistance $R_F(0)$, and the ratio of the short to the “working” wire resistance $R_S(0)/R_W(0)$, all at zero time, are required. It is not possible to obtain all the necessary measurements from a single run. First, a transient run is performed to measure the out-of-balance voltage and the supply voltage, and then a steady-state run is carried out to determine the values of the bridge resistances at zero time.

The application of a voltage across the hot wires, which is necessary when making a measurement, makes the measurement of the initial resistances (i.e., at $t=0$) of the wires difficult. To overcome this problem a

steady-state run follows the transient run. This involves the application of three pre-set supply voltages: 0.5, 1.0, and 1.5 V and the measurement of the voltages across various bridge resistors. The data are stored and are later treated. It can be shown that it is possible to fit and extrapolate the data set by a process of linear regression in order to obtain the value at zero voltage of the resistances of three elements of the bridge. The voltage is measured across points (Fig. 2) AB, AC, AD, AE, and AF. From a single circuit analysis, the following relationships can be written:

$$\frac{V_{AB}}{V_S} = \frac{R_{Std}}{\Sigma R(0)} \quad \frac{V_{AC}}{V_S} = \frac{R_{Std} + R_2}{\Sigma R(0)} \quad (11)$$

$$\frac{V_{AD}}{V_S} = \frac{R_F(0)}{\Sigma R(0)} \quad \frac{V_{AE}}{V_S} = \frac{R_F(0) + R_S(0) + R_1}{\Sigma R(0)} \quad (12)$$

$$V_{AF} = V_S \quad (13)$$

Hence, the values of the unknown resistances $\Sigma R(0)$, $R_F(0)$, $R_L(0)$, $R_S(0)$, R_1 and R_2 are calculated from the known value of the standard resistor R_{Std} . Values of lead resistance are measured during the assembly of the wires.

4. MEASUREMENTS

A measurement of the thermal conductivity is accomplished in the following manner. The bridge is balanced, and the transient run is started by the application of the voltage and the consequent recording of the out-of-balance points up to the required time. About 500 to 1000 such readings are automatically recorded. Following that, the steady-state measurements are automatically performed. From the bridge equation, Eq. (3), for every specific time, the resistance change can be obtained, and thus the corresponding temperature rise via Eq. (8). In this way, the full experimental temperature rise vs. time curve is obtained. This curve should be identical with the curve produced by the solution of the equations, in Table AII of Appendix A, by the finite-element analysis. The only unknowns in the latter case are the thermal conductivity and the (ρC_p) of the material. Hence, by superimposing the two curves (experimental and finite-element predicted), the thermal conductivity and the (ρC_p) of the material are obtained. These two quantities are obtained by trial and error; we note however that the value of the thermal conductivity mostly affects the slope of the curve while the product (ρC_p) results in a vertical shift.

The temperature and time uncertainty produce an error of much less than 0.1% to the final value of the thermal conductivity. No theoretical approximations are made. The uncertainty of the measurements is estimated

to be better than $\pm 1\%$ as derived from the sensitivity of the thermal conductivity value to the superimposition of the experimental and predicted curves. In general, it is noteworthy that the thermal conductivity of the solid material influences the slope of the whole curve, while the changes in the product (ρC_p) produces a shift of the curve parallel to the temperature axis. The uncertainty associated with the evaluation of the product (ρC_p) for the solid is 3%. This illustrates that the use of an absolute rigorous theory has the advantage of yielding the product (ρC_p) of the solid material as well as its thermal conductivity.

4.1. Validation of Technique

An advantage of the proposed configuration is that, it can also be employed to measure the thermal conductivity of fluids. Liquid toluene has been proposed by the Subcommittee on Transport Properties of the International Union of Pure and Applied Chemistry as a standard with an uncertainty of 0.5% [16].

In this case, the sensor was placed in toluene at 295.15 K, and the equations were solved with the intermediate and solid layers substituted by liquid toluene. In Fig. 3 we can see the temperature rise. For this run 500 readings were employed from 0 to 1 s, with a temperature rise of 5 K. As can be seen, the experimental and predicted FEM curves coincide for the values $\lambda = 0.1301 \text{ W} \cdot \text{m}^{-1} \cdot \text{K}^{-1}$ and $(\rho C_p) = 1.47 \times 10^6 \text{ J} \cdot \text{m}^{-3} \cdot \text{K}^{-1}$ for toluene. The equivalent recommended values [16] are $\lambda = 0.1305$

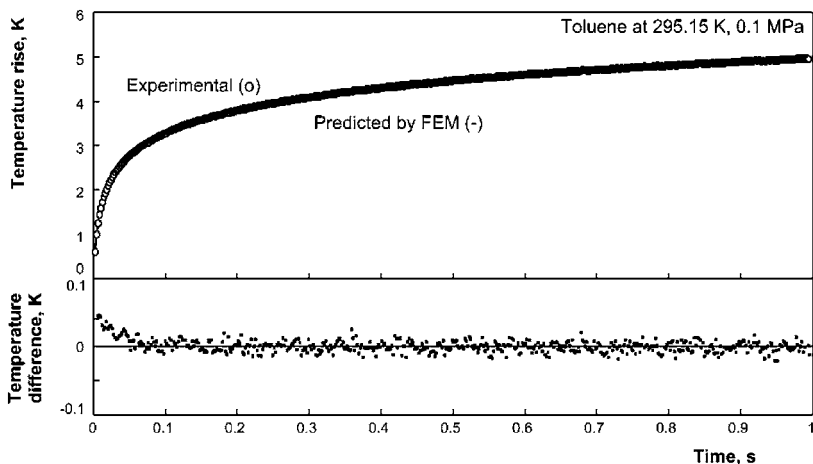


Fig. 3. Experimental and predicted temperature rise in toluene.

$\text{W} \cdot \text{m}^{-1} \cdot \text{K}^{-1}$ and $(\rho C_p) = 1.47 \times 10^6 \text{ J} \cdot \text{m}^{-3} \cdot \text{K}^{-1}$. This confirms our observations that the method can determine the thermal conductivity in an absolute way with an uncertainty of better than $\pm 1\%$, and the product (ρC_p) with 3%.

4.2. Ceramic Material

The sensor with the two wires was subsequently placed between two pieces of Pyroceram 9606. This material is a glassy ceramic, originally developed by NASA, and since it is particularly well defined and thermally stable, it is a certified reference material for thermal conductivity by the National Institute of Standards and Technology, U.S.A., and a currently considered a candidate by the National Physical Laboratory, U.K. Its thermal conductivity had been calibrated by Anter Corporation, USA, $\lambda_s = 3.995 \text{ W} \cdot \text{m}^{-1} \cdot \text{K}^{-1}$. Its density, ρ_s , was found to be equal to $2596 \text{ kg} \cdot \text{m}^{-3}$, and its specific heat capacity, C_{ps} , is $788 \text{ J} \cdot \text{kg}^{-1} \cdot \text{K}^{-1}$ (Anter Corporation, USA). The pieces of $10 \times 5 \times 2 \text{ cm}^3$ were kept in place by a weight over them, and were maintained at 298.15 K , while the air gap between them was $30 \mu\text{m}$. With this setup the temperature rise was recorded for 20 s. The theoretical calculation shown in Fig. 4 assumes perfect thermal contact between the wire and the ceramic and the known values of the properties of the pyroceram. It can be seen that the two curves differ in temperature rise by more than a factor of 2 at long times. Detailed analysis demonstrates that this is entirely due to the very different slope at small times, which arises from the existence of an air gap in the experimental arrangement. No

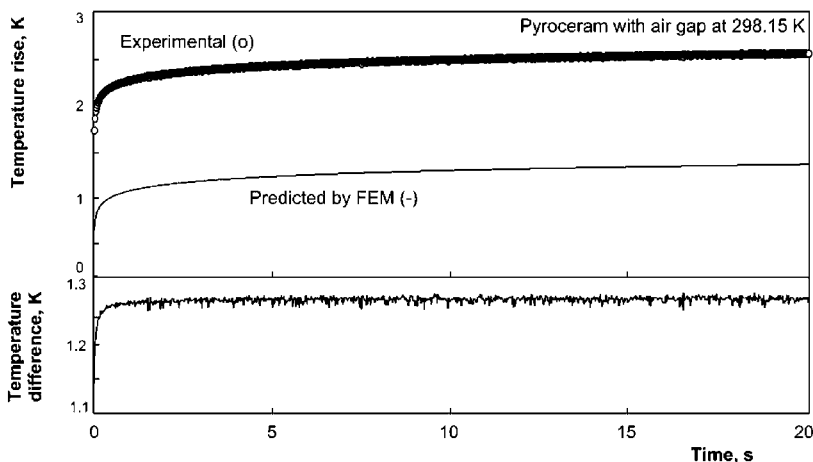


Fig. 4. Experimental and predicted temperature rise in pyroceram (with air gap).

realistic adjustment of the properties of the solid can bring the theoretical and experimental curves into coincidence.

The aforementioned phenomenon has been observed by many workers in the field. The proposed solution has been to fill the air gap with powder from the material. Since the pyroceram is a hard material, this idea was tried with a softer ceramic (IEC 672-3, Ceram CA'B Slovakia). In this case the gap was filled by powder from the ceramic and a weight was placed over it. In Fig. 5, a similar situation is observed. The temperature difference between the two curves is reduced by adding powder, but they are still 0.9 K apart.

In order to eliminate any remaining contact resistance, the gap between the wire and the ceramic was filled with a silicone paste (heat transfer compound, HTCO2S, Electrolube). A further advantage is that the measurement can now be achieved in the following way:

- At small times ($t < 0.15$ s) the heat wave generated is confined to the paste. Since the bridge can be operated from 20 μ s, we can employ it at this time interval to obtain the unknown properties of the paste.
- Having obtained these, at larger times we can solve for the two layers for the properties of the pyroceram.

Indeed, in Fig. 6, the experiment only up to 0.12 s is shown to obtain the properties of the silicone paste. The two curves coincide for the values $\lambda_m = 0.4707 \text{ W} \cdot \text{m}^{-1} \cdot \text{K}^{-1}$ and $(\rho_m C_{pm}) = 1.08 \times 10^6 \text{ J} \cdot \text{m}^{-3} \cdot \text{K}^{-1}$ for the silicone paste. With these values, in Fig. 7, a measurement in pyroceram with

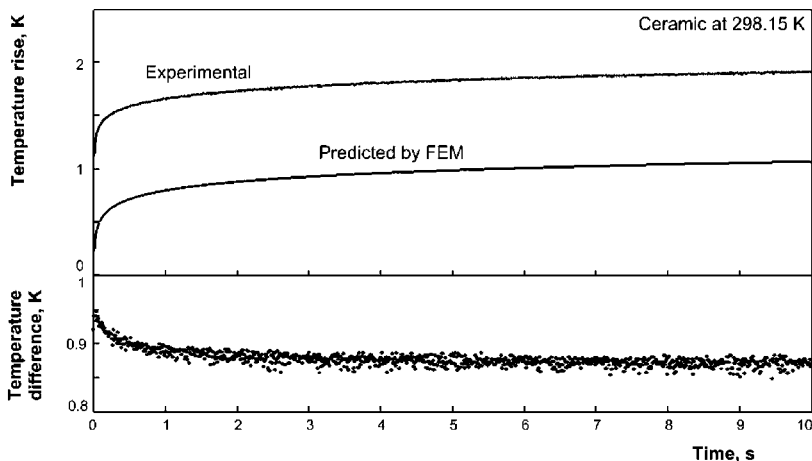


Fig. 5. Experimental and predicted temperature rise in ceramic (with gap filled with powder).

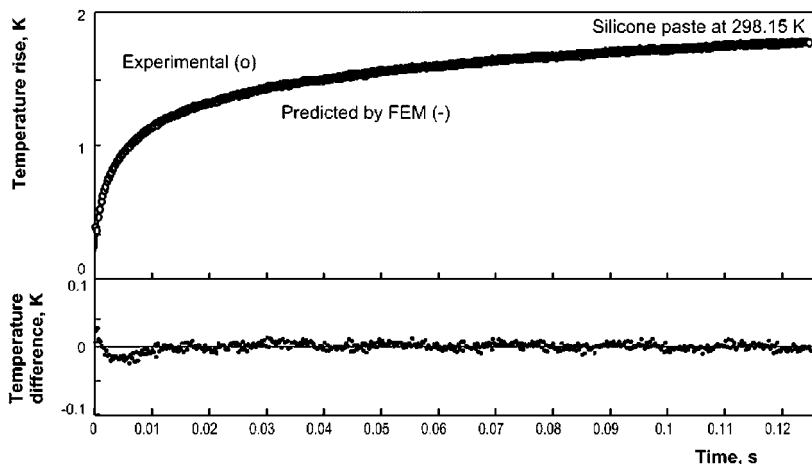


Fig. 6. Experimental and predicted temperature rise in silicone paste.

silicone paste is shown. The only unknowns here were, the thickness of the silicone paste layer and the properties of the pyroceram. The values obtained were $\lambda_S = 4.005 \text{ W} \cdot \text{m}^{-1} \cdot \text{K}^{-1}$ and $(\rho_S C_{pS}) = 2.086 \times 10^6 \text{ J} \cdot \text{m}^{-3} \cdot \text{K}^{-1}$ (actually $C_{pS} = 803.7 \text{ J} \cdot \text{kg}^{-1} \cdot \text{K}^{-1}$, $\rho_S = 2596 \text{ kg} \cdot \text{m}^{-3}$ as the sample was weighted). As already stated, this sample of pyroceram is a reference material with $\lambda = 3.995 \text{ W} \cdot \text{m}^{-1} \cdot \text{K}^{-1}$ and $C_p = 788 \text{ J} \cdot \text{kg}^{-1} \cdot \text{K}^{-1}$. Hence, we see that the proposed method is able to measure the thermal conductivity with very small uncertainty.

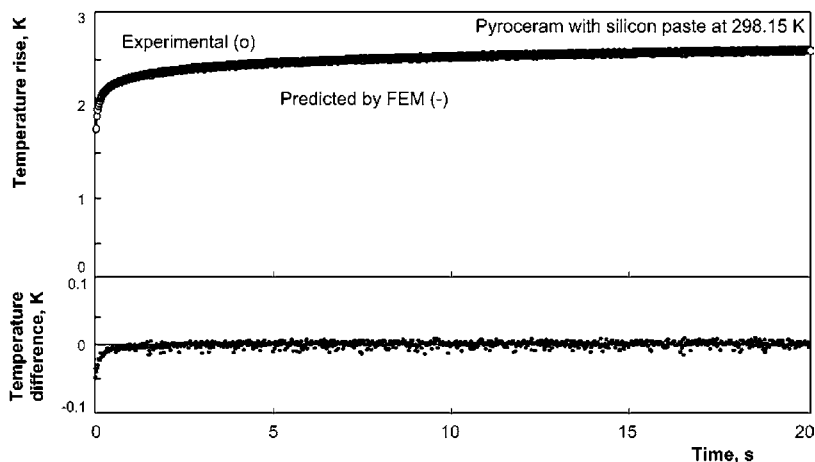


Fig. 7. Experimental and predicted temperature rise in pyroceram (with silicon paste).

5. CONCLUSIONS

A novel application of the transient hot-wire technique has been described. The wires placed in a soft silicone paste between the ceramic material allow, at very small times, the calculation of the unknown properties of the soft paste and with these values, at larger times, the calculation of the thermal conductivity and the product (ρC_p) of the ceramic material. The method is based on a full theoretical model with equations solved by finite elements for the exact geometry. The uncertainty achieved for the thermal conductivity is better than $\pm 1\%$, and for the product (ρC_p) is about 3% .

It should further be noted that, the whole measurement take place in about 10 to 20 s, during which the temperature rise is less than 4 K.

APPENDIX A: THE WORKING EQUATIONS

Table AI. Working Equations

Equations	
Tantalum wire	$\rho_w C_{pw} \frac{\partial T_w}{\partial t} = \lambda_w \left[\frac{\partial^2 T_w}{\partial x^2} + \frac{\partial^2 T_w}{\partial y^2} \right] + \frac{q}{a^2}$
Intermediate layer	$\rho_m C_{pm} \frac{\partial T_m}{\partial t} = \lambda_m \left[\frac{\partial^2 T_m}{\partial x^2} + \frac{\partial^2 T_m}{\partial y^2} \right]$
Solid	$\rho_s C_{ps} \frac{\partial T_s}{\partial t} = \lambda_s \left[\frac{\partial^2 T_s}{\partial x^2} + \frac{\partial^2 T_s}{\partial y^2} \right]$
Solved subject to the following boundary and initial conditions:	
Boundary conditions	
(1) Wire-Intermediate layer interface: $y = \pm \frac{a}{2}$, $x = 0$ to $\pm \frac{a}{2}$; $x = \pm \frac{a}{2}$, $y = 0$ to $\pm \frac{a}{2}$	
$T_w = T_m, \quad \lambda_w \frac{\partial T_w}{\partial x} = \lambda_m \frac{\partial T_m}{\partial x} \quad \text{and} \quad \lambda_w \frac{\partial T_w}{\partial y} = \lambda_m \frac{\partial T_m}{\partial y} \quad t > 0$	
(2) Intermediate layer—Solid interface: $y = \pm \delta$, $x = 0$ to $\pm \frac{b}{2}$	
$T_m = T_s, \quad \lambda_m \frac{\partial T_m}{\partial x} = \lambda_s \frac{\partial T_s}{\partial x} \quad \text{and} \quad \lambda_m \frac{\partial T_m}{\partial y} = \lambda_s \frac{\partial T_s}{\partial y} \quad t > 0$	
(3) $x = \infty$ or $y = \infty$ $T_w = T_m = T_s = T_0 \quad t > 0$	
Initial condition	
(4) $t = 0$ $T_w = T_m = T_s = T_0$ any x, y	

Table AII. Working Equations in Dimensionless Form

Dimensionless variables	
$T^* = (T - T_0) \frac{\lambda}{q}, \quad t^* = \frac{k_w}{a^2} t \quad \text{where} \quad k_w = \frac{\lambda_w}{\rho_w C_{pw}} \quad \text{and} \quad x^* = \frac{x}{a}, \quad y^* = \frac{y}{a}$	
Equations	
Tantalum wire	$\frac{\partial T_w^*}{\partial t^*} = \left[\frac{\partial^2 T_w^*}{\partial x^{*2}} + \frac{\partial^2 T_w^*}{\partial y^{*2}} \right] + 1$
Intermediate layer	$\frac{\rho_m C_{pm}}{\rho_w C_{pw}} \frac{\partial T_m^*}{\partial t^*} = \frac{\lambda_m}{\lambda_w} \left[\frac{\partial^2 T_m^*}{\partial x^{*2}} + \frac{\partial^2 T_m^*}{\partial y^{*2}} \right]$
Solid	$\frac{\rho_s C_{ps}}{\rho_w C_{pw}} \frac{\partial T_s^*}{\partial t^*} = \frac{\lambda_s}{\lambda_w} \left[\frac{\partial^2 T_s^*}{\partial x^{*2}} + \frac{\partial^2 T_s^*}{\partial y^{*2}} \right]$
Solved subject to the following boundary and initial conditions:	
Boundary conditions	
(1) Wire-Intermediate layer interface: $y^* = \pm \frac{1}{2}, x^* = 0 \text{ to } \pm \frac{1}{2}; x^* = \pm \frac{1}{2}, y = 0 \text{ to } \pm \frac{1}{2}$	
$T_w^* = T_m^*, \quad \frac{\partial T_w^*}{\partial x^*} = \frac{\partial T_m^*}{\partial x^*} \frac{\lambda_m}{\lambda_w} \quad \text{and} \quad \frac{\partial T_w^*}{\partial y^*} = \frac{\partial T_m^*}{\partial y^*} \frac{\lambda_m}{\lambda_w} \quad t^* > 0$	
(2) Intermediate layer—Solid interface: $y^* = \pm \frac{\delta}{a}, x^* = 0 \text{ to } \pm \frac{b}{2a}$	
$T_m^* = T_s^*, \quad \frac{\partial T_m^*}{\partial x^*} = \frac{\partial T_s^*}{\partial x^*} \frac{\lambda_s}{\lambda_m} \quad \text{and} \quad \frac{\partial T_m^*}{\partial y^*} = \frac{\partial T_s^*}{\partial y^*} \frac{\lambda_s}{\lambda_m} \quad t^* > 0$	
(3) $x^* = \infty$ or $y^* = \infty$ $T_w^* = T_m^* = T_s^* = T_0^* \quad t^* > 0$	
Initial condition	
(4) $t^* = 0 \quad T_w^* = T_m^* = T_s^* = T_0^* \quad \text{any } x, y$	

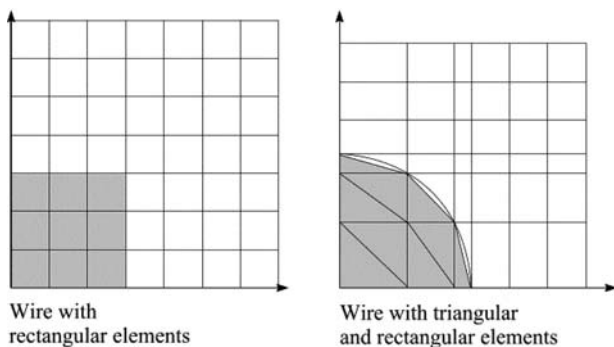


Fig. B1. Representation of the circular wire with two different meshes.

APPENDIX B

In order to establish the suitability of the representation of the circular wire as a mesh of rectangular elements, a test with liquid toluene was carried out. The results were analysed with two different types of meshes, as shown in Fig. B1. Although the second mesh, is a much better representation of the circular wire, the data obtained, produced the same value of the thermal conductivity within its uncertainty. Hence, the first arrangement was preferred due to its speed of conversion.

REFERENCES

1. M. J. Assael, M. Dix, A. Lucas, and W. A. Wakeham, *J. Chem. Soc., Faraday Trans. 1* 77:439 (1981).
2. E. Charitidou, M. Dix, M. J. Assael, C. A. Nieto de Castro, and W. A. Wakeham, *Int. J. Thermophys.* 8:511 (1987).
3. W. A. Wakeham, A. Nagashima, and J. V. Sengers, eds, *Experimental Thermodynamics. Vol. III. Measurements of the Transport Properties of Fluids* (Blackwell Scientific Publications, London, 1991).
4. W. E. Haupin, *Am. Ceram. Soc. Bull.* 39:139 (1960).
5. A. Von Mittenbühler, *Ber. Dtsch. Keram. Ges.* 41:15 (1964).
6. Deutsches Institut für Normung, *Testing of Ceramic Materials: Determination of Thermal Conductivity up to 1600 °C by the Hot-Wire Method. Thermal Conductivity up to 2 W/mK* (in German), DIN 51046 (August 1976).
7. European Committee for Standardization, *Methods of Testing Dense Shaped Refractory Products. Part 14: Determination of Thermal Conductivity by the Hot-Wire (Cross-Array) Method.* EN 993-14 (1998).
8. European Committee for Standardization, *Methods of Testing Dense Shaped Refractory Products. Part 15: Determination of Thermal Conductivity by the Hot-Wire (Parallel) Method.* EN 993-15 (1998).
9. L. Vozár, *J. Therm. Anal.* 46:495 (1996).

10. G. D. Morrow, *Ceram. Bull.* **58**:687 (1979).
11. L. Binkele, *High Temp.-High Press.* **15**:131 (1983).
12. W. R. Davis and A. M. Downs, *Trans. Br. Ceram. Soc.* **79**:44 (1980).
13. S. E. Gustafsson, *Rev. Sci. Instrum.* **62**:797 (1991).
14. M. Dix, I. W. Drummond, M. Lesemann, V. Peralta-Martinez, W. A. Wakeham, M. J. Assael, L. Karagiannidis, and H. R. van den Berg, in *Proc. 5th ATPC* (Seoul, Korea, 1998), p. 113.
15. J. Kestin and W. A. Wakeham, *Phys. A* **92**:102 (1978).
16. M. L. V. Ramires, C. A. Nieto de Castro, R. A. Perkins, Y. Nagasaka, A. Nagashima, M. J. Assael, and W. A. Wakeham, *J. Phys. Chem. Ref. Data* **29**:133 (2000).